

# Joining Technology That Contributes to Improving the Reliability of Next-generation EV Chassis

Yoshinari ISHIDA\*  
Yuki KITAHARA  
Hiroshi YOSHIDA

Masahiro MATSUBA  
Shinji KODAMA

## Abstract

*This study introduces advancements in arc welding technologies to enhance the reliability of chassis components in next-generation electric vehicles. Key developments include reinforcement beads for improved fatigue strength, high-formability 980 MPa-class steel, and low-slag, low-spatter welding wires for better corrosion resistance. Welding solutions are tailored for arms, links, ladder frames, and subframes to meet the structural demands of electrification. These approaches support both lightweight design and durability, contributing to the evolution of reliable EV chassis structures.*

## 1. Introduction

From the perspective of rapidly advancing emission reduction initiatives, reducing vehicle weight has become an essential challenge. Nippon Steel Corporation has developed solutions for high-performance high-strength steel sheets, as well as for the design, manufacturing, and evaluation of components, meeting these needs through their application.

Within the vehicle body, chassis components—such as arms, links, torsion beams, and other unsprung parts—along with skeletal components like subframes and ladder frames, utilize steel plates that are relatively thicker than other body sections. These components support the power unit and drivetrain while absorbing road input, necessitating long-term durability and rigidity.

In reducing CO<sub>2</sub> emissions during operation, the shift toward electric vehicles is expected to progress long-term.<sup>1,2)</sup> This necessitates vehicle design centered on expensive high-capacity batteries, along with advanced steel sheets and the expertise to utilize them effectively. Key new challenges accompanying electrification include achieving high rigidity and fatigue strength to counter increased vehicle weight, developing collision energy absorption structures for battery protection,<sup>3)</sup> and further reducing component costs beyond conventional levels.

Arc welding is frequently employed for joining chassis components. Compared to resistance spot welding, widely used for body joining, arc welding offers advantages such as the ability to perform continuous welding, facilitating the assurance of member strength

and rigidity; suitability for single-side access welding, ideal for manufacturing closed-section structures; and high adaptability to construction disturbances like plate gaps. However, arc welded joints inherently become stress concentration points due to their structure.<sup>4)</sup> For heavier electric vehicles, measures to enhance the fatigue strength of welded joints are more critical than ever. Furthermore, slag formation on the weld bead surface is unavoidable, potentially causing electrodeposition coating defects and becoming corrosion initiation points.<sup>5)</sup> Therefore, while switching to GA-coated steel sheets is a potential solution from a corrosion resistance perspective, this has not been sufficiently advanced for chassis components. This is because in widely used joint types such as lap joints with fillet welds and T-joints, porosity defects caused by the vaporization of the coating due to welding heat frequently occur, raising concerns about reduced joint strength.<sup>6)</sup>

To apply ultra-high-strength steel sheets to chassis components while suppressing or minimizing plate thickness increases and promoting weight reduction, it is necessary to ensure fatigue strength even more than before, improve corrosion resistance, and expand the application of GA-coated steel sheets. Furthermore, establishing methods to resolve challenges during component manufacturing is considered important. This report introduces recent topics being addressed to enhance the fatigue strength and corrosion resistance of arc welded joints in automotive chassis components and to expand the application of GA-coated steel sheets.

\* Senior Manager, Head of Section, Senior Researcher, Welding & Joining Research Lab., Steel Research Laboratories  
20-1 Shintomi, Futtsu City, Chiba Pref. 293-8511

## 2. Arm Link Component Joining Solutions

Arm and link components are part of the suspension system and are critical for driving performance, ride comfort, and safety. High-strength steel sheets are often used as the material. While open-section structures formed by press forming are used in small and medium-sized vehicles, monocoque structures formed by arc welding are increasingly adopted for small and medium-sized vehicles due to the need for increased rigidity as vehicle weight increases. From a manufacturing cost perspective, weld-free solutions are sought. Methods such as integrated forming utilizing burring for bushing press-fit sections have been proposed.<sup>7)</sup> Furthermore, for lower arms, to address increased vehicle weight due to electrification, partially open-section structures are being investigated. These aim to minimize weld length to reduce manufacturing costs while ensuring strength and rigidity.<sup>8)</sup>

### 2.1 Improving fatigue strength of bush collar welded joints

While the application of open-section lower arms is expected to expand from the perspective of reducing welding costs, challenges remain for achieving completely weld-free construction. For example, the collar into which the bushing is pressed is almost always arc-welded to the arm body. In the example shown in Fig. 1, the bushing collar is butt-welded to a U-shaped formed section extending from the arm body. The joint configuration is a single-sided T-fillet weld. Due to restricted access for the welding torch, the entire butt section cannot be welded, leaving the end of the weld bead exposed. Consequently, stress concentration at the weld bead end and the resulting fatigue crack initiation become critical issues.

Nippon Steel is investigating methods to enhance the fatigue strength of welded joints by optimizing weld bead placement (reinforcing beads). Here, we present a case study targeting the bush collar of the lower arm. A reinforcement weld bead refers to a weld bead applied to a pressed part itself, in addition to the weld bead joining pressed parts together. This partially increases the plate thickness at that location, suppresses bending deformation in the surrounding area, and reduces stress concentration associated with deformation.<sup>9)</sup>

Figure 2 shows the principal stress distribution around the bush collar of the front lower arm when subjected to loads simulating actual vehicle conditions. Figure 2 (a) presents the shell element model of the front lower arm and stiffening bead, (b) shows the detailed shape of the stiffening bead, (c) displays the stress distribution without the stiffening bead, and (d) shows the stress distribution with the stiffening bead.

Without the stiffening bead, high stress of 491 MPa occurs at the weld end. However, adding a stiffening bead originating from this stress concentration point reduces the weld end stress to 357 MPa, a decrease of approximately 20%. Furthermore, by optimizing the

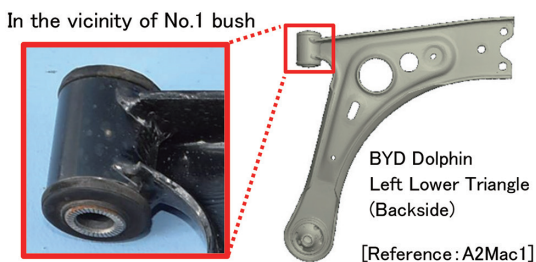


Fig. 1 Joint part of bush collar in open type front lower arm

welding conditions (crater conditions) to create a gentler shape, stress concentration at the stiffening bead's end was also prevented.

Such modifications to weld bead placement, also called sacrificial beads, are sometimes considered as countermeasures when fatigue strength deficiencies in welded areas become apparent during the late stages of actual vehicle development. However, examining countermeasures from the design stage enables development without rework and is expected to contribute to shortening the development schedule.

### 2.2 Welded joint performance of newly developed 980 MPa-class hot-rolled high formability steel sheet

As mentioned earlier, high-strength hot-rolled steel sheets are used for arm and link components. While 780 MPa-class steel sheets are currently the most common, the application of 980 MPa-class steel sheets is increasing. Nippon Steel has developed a 980 MPa-class hot-rolled high-formability steel sheet (hereinafter HR980HF) with good ductility and flange elongation, suitable for arm and link components.<sup>9)</sup> The following presents evaluation results for the fatigue strength and post-painting corrosion resistance of HR980HF welded joints, representing their fundamental performance characteristics, utilizing Nippon Steel's welding technology.

#### 2.2.1 Corrosion resistance of HR980HF welded joints

While there is a high demand for weld-free construction to reduce manufacturing costs, closed-section structures, which are advantageous for ensuring strength and rigidity, are sometimes adopted to counteract the increase in vehicle body weight associated with electrification. Closed-section lower arms are formed by welding together upper and lower parts press-formed into a U-shape. Compared to open-section structures, relatively thin high-strength steel sheets are used. Therefore, ensuring corrosion resistance at the welded joints is critical to prevent wall thinning due to corrosion.

The cause of corrosion at welded joints is poor formation of electrodeposition coating due to non-conductive weld slag. Proposed solutions include low-CO<sub>2</sub> shielding gases<sup>10, 11)</sup> and low-slag

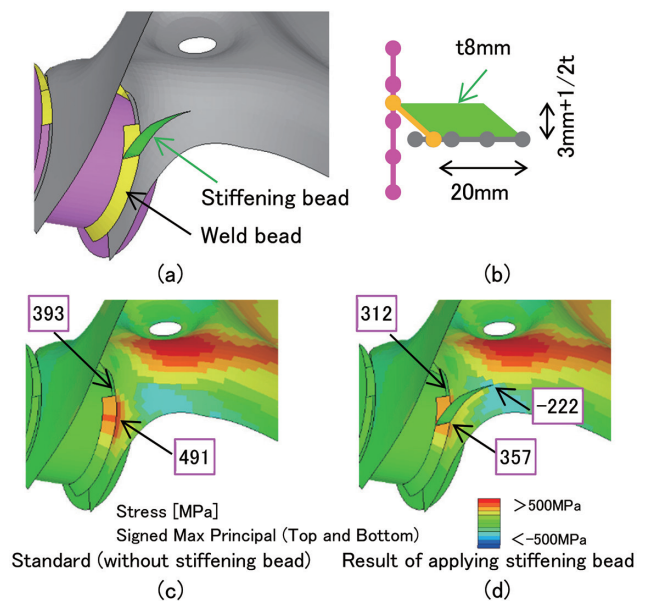


Fig. 2 CAE model around the collar and distribution of maximum principal stress

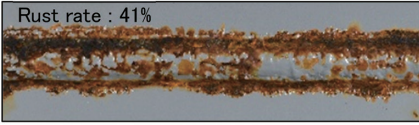
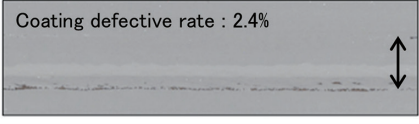
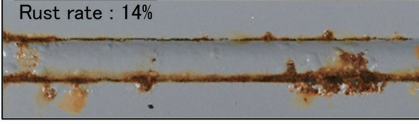
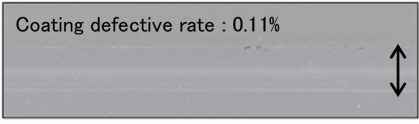
	After electro-deposition coating (Coating thickness=25 μm)	After corrosion test (JASO M609 120cycles)
Standard wire (YM-24T) Standard Shield (Ar+20%CO <sub>2</sub> )	Coating defective rate : 11.6% 	Rust rate : 41% 
Low-slag wire (YM-TX) Standard Shield (Ar+20%CO <sub>2</sub> )	Coating defective rate : 2.4% 	Rust rate : 14% 
Low-slag wire (YM-TX) Low-CO <sub>2</sub> Shield (Ar+5%CO <sub>2</sub> )	Coating defective rate : 0.11% 	Rust rate : 0.9% 

Fig. 3 Weld bead appearance after electro-deposition coating and the corrosion test

wires<sup>12, 13)</sup> to suppress slag generation, as well as slag removal technologies via post-processing. Nippon Steel has developed the low-slag solid wire “YM-TX”<sup>14)</sup> based on the fundamental concepts of minimizing slag generation through Si-free weld wire composition and imparting conductivity to the slag. This wire has already been adopted by customers.

Figure 3 shows the appearance of the welded area of HR980HF (plate thickness 2.6 mm) after electrodeposition coating and after a combined cycle corrosion test. Lap fillet welds were made using DC pulse welding mode, comparing the effects of standard wire (YM-24T), low-slag wire (YM-TX), and the CO<sub>2</sub> mixture ratio in the shielding gas. The coating defect rate was defined as the area of coating defects divided by the weld bead area after electrodeposition coating. The red rust area rate was defined as the red rust area divided by the weld bead area after corrosion testing.

The coating defect rate for the standard wire exceeded 10%, whereas it decreased to about 2% for the low-slag wire (YM-TX). Furthermore, when the shielding gas was Ar+5% CO<sub>2</sub>, the coating defect rate fell below 1%. Additionally, the red rust occurrence rate for the low-slag wire was approximately one-third that of the standard wire. Moreover, reducing the CO<sub>2</sub> mixture ratio in the shielding gas significantly decreased the red rust area ratio.

Figure 4 shows SEM images of the electrodeposited coating film formation area and CITS (Current Imaging Tunneling Spectroscopy) images obtained using a scanning probe microscope.<sup>15)</sup> CITS indicates the current intensity at each measurement point, serving as an indicator of conductivity. Slag from the coating defect area, investigated separately, was primarily amorphous Si-Mn-based oxides and showed no conductivity whatsoever. However, the slag in the coating formation area was composed of multiple oxides and was identified as Mn<sub>2</sub>TiO<sub>4</sub>. This confirmed that this Mn-Ti-based oxide contributes to the conductivity of the slag, which is necessary for the formation of the electrodeposition coating.

### 2.2.2 Fatigue strength of HR980HF welded joints

Factors affecting the fatigue strength of arc welds include residual welding stresses, stress concentration due to geometry, and the microstructure at crack initiation sites. Methods to enhance fatigue strength include introducing compressive residual stresses via shot peening or ultrasonic impact treatment (UIT),<sup>16)</sup> plasma-arc hybrid

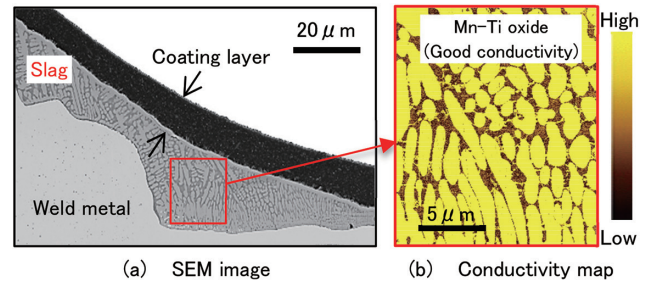


Fig. 4 SPM analysis result of slag cross section

welding techniques,<sup>10, 17)</sup> the “MX-MIG” process,<sup>18)</sup> and other arc welding processes that produce a flat weld bead shape, as well as increasing the strength of the welding wire.<sup>5)</sup>

However, all these methods increase manufacturing costs and have not been widely adopted for automotive parts. Therefore, fatigue strength improvement measures based on existing production processes and equipment, such as the aforementioned stiffening beads, are desired.

Here, to evaluate the fatigue strength improvement effect of HR980HF as an advantage, low-slag wire (YM-TX) was used for the welding wire from the perspective of ensuring corrosion resistance at the welded joint, and fatigue strength was assessed using a plane bending fatigue test on lap fillet weld.<sup>19)</sup> Figure 5 shows a comparison of the fatigue strength of welded joints in conventional 980 MPa-class hot-rolled steel sheets (hereinafter HR980) and HR980HF. Comparing HR980 and HR980HF, despite equivalent weld bead shapes, the stress amplitude at the 2 million cycle fatigue limit increased from 175 MPa to 200 MPa, and the fatigue life around 250 MPa also increased approximately twofold. Furthermore, when using Ar+5% CO<sub>2</sub> as the shielding gas for HR980HF, the weld toe exhibited a smoother shape compared to Ar+20% CO<sub>2</sub>, demonstrating a significant improvement in fatigue strength.

## 3. Ladder Frame Joining Solutions

Ladder frame vehicles tend to be used in harsher environments than monocoque vehicles and also have longer service lives and higher mileage. Therefore, ladder frames require not only strength and rigidity but also high fatigue durability. Consequently, the plate

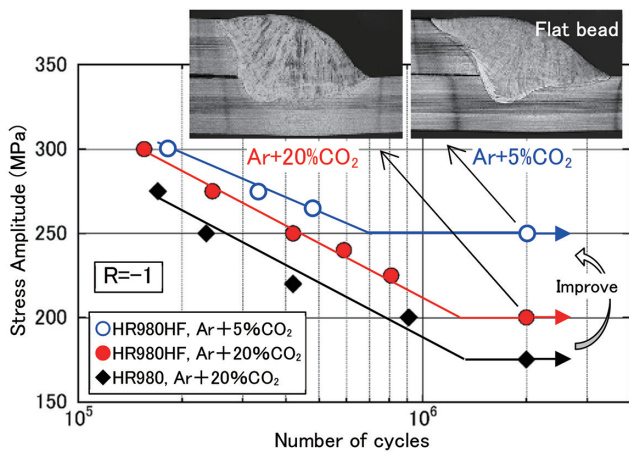


Fig. 5 S-N characteristics of 980 MPa-class hot-rolled steel sheet

thickness of side frames and cross members is thick, and reinforcements are added in various locations, sometimes causing the total weight of the ladder frame to reach 300 kg or more. Therefore, the expected effect of weight reduction through plate thickness reduction and reinforcement reduction is significant. Consequently, measures such as adopting nonlinear TWB structures via laser-arc hybrid welding, reducing weight equivalent to the overlap allowance through butt welding, and strategically employing ultra-high-strength steel sheets are being implemented.<sup>20, 21)</sup> With the electrification of ladder frame vehicles, the structure has undergone significant changes, such as reducing the number of cross members under the cabin to secure battery mounting space.<sup>22, 23)</sup> Consequently, requirements for fatigue properties at the cross member-side member joints have increased. This may lead to weight increases due to thicker plates or the addition of new lower frames.

Therefore, to reduce stresses at the cross member-side member joint and improve fatigue properties, the effectiveness of the stiffening beads described in Section 2.1 was investigated. Figure 6(a) shows the analysis model and boundary conditions. Using the publicly available analysis model of the 2014 Chevrolet Silverado,<sup>24)</sup> we compared the maximum principal stresses at the cross member-side member joint when applying an upward load to the right front suspension tower. We focused on two representative joint locations: the

bend section of the weld bead (① in the figure) and the notch section of the cross member (② in the figure).

Figure 6(b) compares the distribution of maximum principal stress at the focus locations before and after applying stiffening beads, showing the reduction effect as a percentage. The stiffening beads were applied starting from the point of maximum principal stress in the original model and extending in the direction of that maximum stress. At evaluation point ①, the cross member is positioned to abut the side member's side surface. The maximum principal stress occurs at the weld bead bend, and applying the stiffening bead reduced this maximum stress to 78%. At evaluation point ②, the top surface of the notched cross member overlaps the top surface of the side member, causing the weld bead to break. The point of maximum principal stress was at the end of the interrupted weld bead. Applying the stiffening bead reduced the stress to 72% even at the highest point, confirming the effectiveness of the stiffening bead here as well. Thus, stiffening beads can effectively reduce stresses around arc welds when placed appropriately. They are considered an effective technology for addressing fatigue reliability issues caused by increased vehicle weight and structural changes associated with electrification.

#### 4. Subframe Joining Solutions

Subframes require various characteristics depending on performance demands such as suspension type, drive system, and vehicle class, yet relatively thin steel sheets are often used. Consequently, restrictions are placed on the thickness of the applied steel sheets from a rust prevention perspective, and measures such as using galvanized steel sheets for salt damage specifications (e.g., for North American markets) are implemented. Furthermore, to protect the battery, the front subframe is evolving into a structure adapted for electrification, incorporating additional impact-absorbing structures like a secondary bumper and crash box. To address these changes, Nippon Steel has developed ultra-high-strength cold-rolled and GA-coated EA steel sheets that offer both excellent impact absorption energy and formability.<sup>9)</sup>

##### 4.1 Selection of welding wire considering hydrogen embrittlement characteristics at welded joints

When applying ultra-high-strength steel sheets, attention must be paid to hydrogen embrittlement cracking in welded joints. Partic-

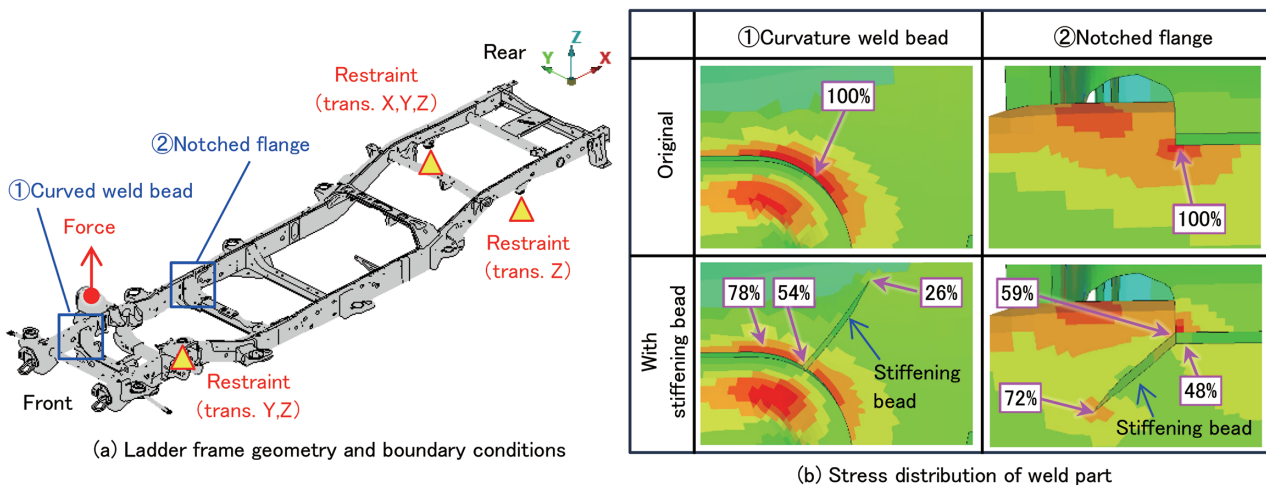


Fig. 6 Effect of applying stiffening bead to ladder frames

ularly in arc welding, hydrogen can infiltrate the weld zone due to the plasma generated during welding, which can dissociate rust-preventive oils on the steel sheet or moisture in the atmosphere. The typical diffusible hydrogen content during standard arc welding is 1 to 1.5 ppm, which is higher than that in resistance spot welding, commonly used for body panels. For welding thick plates in structures like bridges and pressure vessels, hardness standards for welds to suppress hydrogen embrittlement (e.g., Vickers hardness  $\leq 350^{25}$ ) have been established, and ultra-low-hydrogen wires<sup>26)</sup> have been developed to prevent hydrogen embrittlement. On the other hand, while welding subframes, where 590–780 MPa-class steel sheets were mainstream, could be performed without special attention to hydrogen embrittlement, considering the application of 980 MPa-class steel sheets and even 1180 MPa-class steel sheets, it is considered necessary to evaluate their application based on an understanding of hydrogen embrittlement characteristics. The following section introduces Nippon Steel’s hydrogen embrittlement evaluation case studies and presents welding wires suitable for high-strength thin steel sheets.

**Figure 7** shows the hydrogen embrittlement cracking characteristics of lap fillet welds using 980 MPa-class steel sheet. As an indicator of hydrogen embrittlement, the  $P_C$  value was used, referencing thick plate welding.<sup>25)</sup>

$$P_{CM}(\%) = C + Si/30 + Mn/20 + Cu/20 + Ni/60 + Cr/20 + Mo/15 + V/10 + 5B \quad (1)$$

$$P_C = P_{CM} + t/600 + H/60 \quad (2)$$

The  $P_C$  value was calculated from the  $P_{CM}$  derived from the weld metal’s chemical composition, plate thickness  $t$ , and diffusible hydrogen content  $H$ .  $P_{CM}$ ,  $t/600$ , and  $H/60$  represent the weld metal’s susceptibility to hydrogen embrittlement, restraint level, and the effect of diffusible hydrogen, respectively.

As the  $P_C$  value increases, the risk of cracking rises, with cracking occurring at values around 0.3 or higher. In y-type weld crack tests on thick plates, the crack rate increases at  $P_C$  values of approximately 0.3 or higher, generally consistent with the results of this evaluation on thin steel sheet lap joints.

**Figure 8** shows examples of tensile strength for lap fillet welds. During tensile loading, fractures occurred not in the weld metal itself but in the base metal away from the weld metal or in the heat-affected zone near the weld metal, such as the weld toe edge or root area, due to deformation caused by misalignment between the centers of the upper and lower plates’ thicknesses. From the perspective of ensuring high joint strength and suppressing the  $P_C$  value, it is considered desirable to select welding wire designed for 590 MPa-class steel sheets even for ultra-high-strength steel sheets.

#### 4.2 Splatter-reduced low-slag wire

Subframe plate thickness tends to be thinner compared to arms or ladder frames. Therefore, low-heat-input welding conditions with reduced current are applied to prevent welding defects such as burn-through during arc welding. While low-slag wire is considered desirable to improve the corrosion resistance of the welded area, it tended to increase spatter during low-heat-input welding.

**Figure 9** shows an example of evaluating the corrosion resistance after painting of a welded joint with spatter adhesion. The electrodeposition coating on spatter-adhered areas becomes thinner compared to flat areas, making these spatter-adhered areas prone to becoming the starting point for red rust. Removing spatter requires significant labor, so low-spatter low-slag wire was desired from the perspectives of both weld corrosion resistance and reducing welding

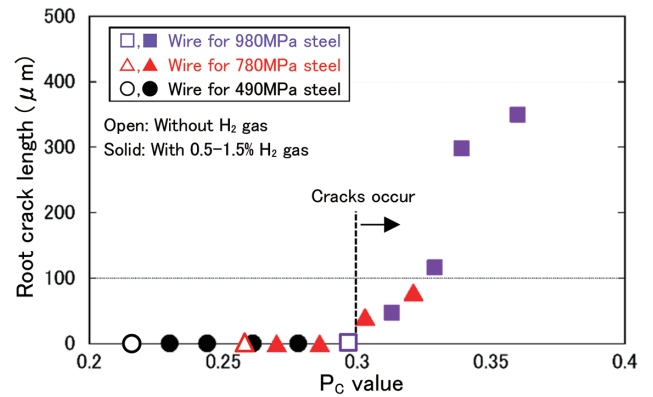


Fig. 7 Effect of  $P_C$  value on root crack length

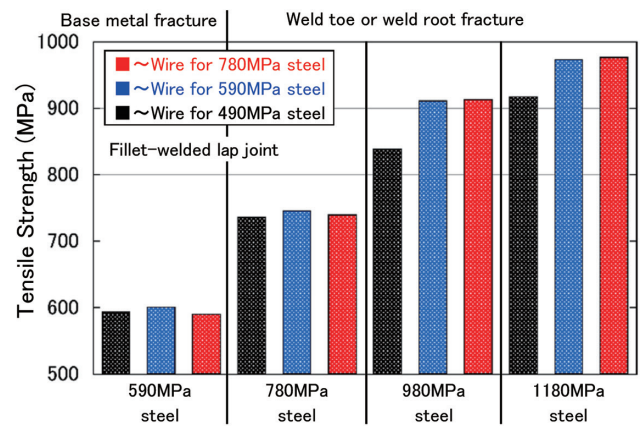
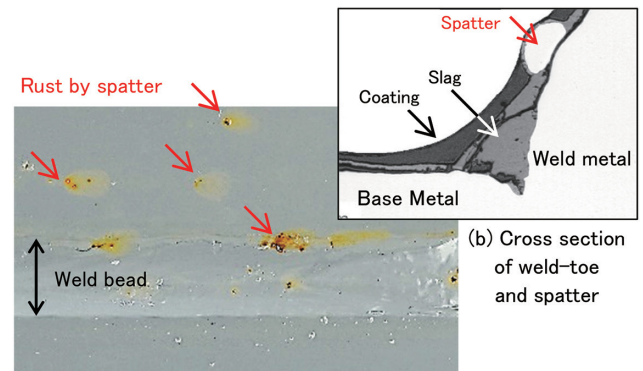


Fig. 8 Tensile strength of lap fillet welds



(a) Appearance of rust by spatter

Fig. 9 Appearance of welded part with spatter after corrosion test

construction costs.

Therefore, a low-slag, low-spatter wire was developed that suppresses spatter generation during low heat input welding with low-slag wire. **Figure 10** shows an example of the spatter reduction effect. Bead-on-plate welding was performed on a flat plate at a welding current of 200 A using DC pulse welding mode with Ar+20% CO<sub>2</sub> as the shielding gas. A plate blocking the arc light was placed in front, and the first 5 seconds after welding initiation were captured with a digital camera. Image processing, such as edge enhancement, was applied to compare the trajectories of scattered spatter. Although the low-slag wire produced more spatter than the

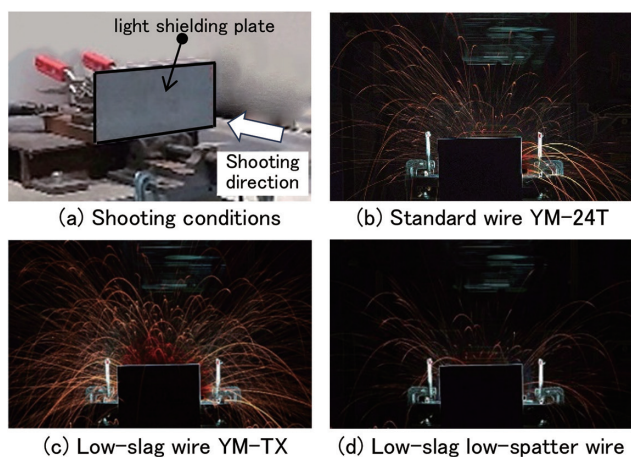


Fig. 10 Comparison of spatter scattering conditions

standard wire, the low-slag, low-spatter wire significantly reduced spatter dispersion, approaching the level of the standard wire. Note that in this evaluation, the pulse waveform of the current was left at the welding power source's default setting. However, by optimizing the waveform—such as the pulse peak current and duration—it is possible to further reduce spatter dispersion to a level where replacing the standard wire poses no significant issues.

## 5. Conclusion

This paper outlined recent initiatives in welding technologies for arm link components, ladder frames, and subframes as electrification-responsive technologies for automotive chassis parts. While improving the corrosion resistance and fatigue strength of arc welded joints is a common elemental technology for all these components, meeting the increasingly demanding requirements for higher strength and thinner sheets necessitates not only material technology but also continuous proposals for low-cost, highly reliable compo-

nents that delve into production processes and part geometries. Going forward, we aim to contribute to automotive weight reduction by realizing reliable joints that leverage the advantages of arc welding and by proposing new construction methods through the development of novel joining processes.

## References

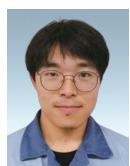
- 1) Xuelian Li: Marubeni Institute Report. April 30, 2025
- 2) Nishimura, K. et al.: Ministry of Finance, The Finance. (710), 69 (2025/01)
- 3) Okamura, J. et al.: SUBARU Technical Review. (49), 39 (2022)
- 4) Seto, A. et al.: Shinnittetsu Giho. (393), 55 (2012)
- 5) Kodama, S. et al.: Nippon Seitetsu Giho. (412), 78 (2019)
- 6) Yamazaki, K.: Japan Welding Engineering Society, Welding Technology Information Center, WE-COM Magazine. (11), (2014/01)
- 7) Volkswagen ID.3 (2020) A2Mac1: <https://ibp.a2mac1.com/data/product/000000AN8AYLEU02>
- 8) Ohtsuka, K. et al.: Nippon Seitetsu Giho. (425), 68 (2025)
- 9) Hironaka, S. et al.: Nippon Seitetsu Giho. (425), 15 (2025)
- 10) Kitani, Y. et al.: JFE Giho. (41), 55 (2018)
- 11) Tanaka, M. et al.: Mazda Technical Review. (41), 172 (2025)
- 12) Kinashi, H. et al.: R&D Kobe Steel Engineering Reports. 72 (1), 79 (2023)
- 13) Furukawa, N. et al.: R&D Kobe Steel Engineering Reports. 73 (2), 88 (2024)
- 14) Iwakami, T.: Nippon Steel Welding & Engineering, Biido. (69), 8 (2020)
- 15) Yoshimura, M.: Oyo Buturi. 79 (4), 336 (2010)
- 16) Nose, T.: Journal of the Japan Welding Society. 77 (3), 6 (2008)
- 17) Kataoka, T. et al.: JFE Giho. (34), 64 (2014)
- 18) Suzuki, R. et al.: R&D Kobe Steel Engineering Reports. 63 (1), 60 (2013)
- 19) Kodama, S. et al.: Shinnittetsu Sumikin Giho. (409), 63 (2017)
- 20) Moritsu, K. et al.: Toyota Technical Review. 70 (1), 34 (2024)
- 21) Era, T. et al.: Japan Welding Engineering Society LMP Symposium 2025
- 22) Ford Authority: <https://fordauthority.com/2022/06/2022-ford-f-150-lightning-frame-live-photo-gallery/>
- 23) Chevrolet Silverado EV: <https://www.chevrolet.com/electric/silverado-ev>
- 24) Center for Collision Safety and Analysis: <https://www.ccsa.gmu.edu/models/2014-chevrolet-silverado/>
- 25) Kasuya, T.: Journal of the Japan Welding Society. 70 (6), 32 (2001)
- 26) Saito, M.: Nippon Steel Welding & Engineering, Biido. (76), 9 (2023)



Yoshinari ISHIDA  
Senior Manager, Head of Section  
Senior Researcher  
Welding & Joining Research Lab.  
Steel Research Laboratories  
20-1 Shintomi, Futtsu City, Chiba Pref. 293-8511



Masahiro MATSUBA  
Manager  
Quality Management Div.  
Nagoya Works



Yuki KITAHARA  
Integrated Steel-Solution Research Lab.-I  
Steel Research Laboratories



Shinji KODAMA  
Dr.Eng., Chief Manager, Head of Dept.  
Welding & Joining Research Lab.  
Steel Research Laboratories



Hiroshi YOSHIDA  
Dr.Eng., General Manager, Head of Lab.  
Welding & Joining Research Lab.  
Steel Research Laboratories